Tara gum-bovine sodium caseinate acid gels: stabilization of W/W emulsions

Hidalgo, Ma. Eugenia [1, 2, *]; Ingrassia, Romina [1, 2, 3]; Nielsen, Nadia Sol [1]; Porfiri, Ma. Cecilia [2, 4]; Daniel Tapia-Maruri [5]; Risso, Patricia Hilda [1, 2, 3]

[1] Facultad de Ciencias Bioquímicas y Farmacéuticas, Universidad Nacional de Rosario (UNR), Suipacha 531, Rosario, Argentina

[2] Consejo Nacional de Investigaciones Científicas y Técnicas (CONICET)

[3] Facultad de Ciencias Veterinarias, UNR, Ovidio Lagos y Ruta 33, Casilda, Argentina

[4] Laboratorio de Investigación en Funcionalidad y Tecnología de Alimentos (LIFTA), Universidad Nacional de Quilmes (UNQ), Roque Sáenz Peña 352, Bernal, Buenos Aires, Argentina

[5] Departamento de Biotecnología, Centro de Desarrollo de Productos Bióticos, Instituto Politécnico Nacional. Carretera Yautepec-Jojutla Km 6, Calle CEPROBI N°8, Col. San Isidro, Yautepec, Morelos, México

*_Corresponding Author_. Address: Suipacha 570 (2000) Rosario, Santa Fe, Argentina

Tel: +54 9 3413285216

E-mail: maruhidalgo80@yahoo.com.ar

Abbreviated Running Headline: W/W emulsion stabilized by acid gelation

Abstract

Microstructural, rheological, and textural behaviour of tara gum-bovine sodium caseinate aqueous mixtures and their acid gels were evaluated. Acid gels with different microstructures and texture were obtained. These results can be related to a competition between the protein

acid gelation process and the segregative phase separation. Depending on the concentration ratio of both biopolymers, a continuous protein gel network or a water-in-water emulsion stabilized by acid gelation were observed. These findings may be used to address the development of new food grade gels with different textures and also for the obtention of protein microgels to encapsulate hydrophilic compounds.

Keywords

Microstructure; Texture; Rheology; Colloids; Milk gels; Water-in-water emulsions

INTRODUCTION

Proteins and polysaccharides are the main biopolymers mostly used in food formulations (Norton and Frith 2001). When these biopolymers mixed together, they may show good miscibility and remain in a single phase or repel each other and separate into two distinct phases. Phase separation may be associative (coacervation process) or segregative (thermodynamic incompatibility) (Tolstoguzov 1991; Ghosh and Bandyopadhyay 2012). The final stage of the segregative phase separation, in the absence of gelation, is a system with macroscopically separated phases in which each phase is enriched in one of the two biopolymers (Corredig *et al.* 2011; Stieger and van de Velde 2013). Some authors have postulated that this behaviour is a consequence of the instability of water-in-water (W/W) emulsions, i.e. droplets of one biopolymer distributed in a continuous phase of the other biopolymer, that tend to coalesce quickly (Esquena 2016; Norton and Frith 2001). However, it has been reported that it would be feasible to obtain stable W/W emulsions by the gelation of one of the biopolymers, and thus, preventing coalescence (Stieger and van de Velde 2013; Esquena 2016).

Tara gum (TG) is extracted from the seeds of *Caesalpinia spinosa*, a Leguminosae that grows in Perú, Bolivia and in the northwest of Argentina. TG is a galactomannan described as a skeleton of β-D-mannopyranosyl units linked (1→ 4), with units of side groups of α-D-galactopyranosyl units linked (1→ 6) (Buffington *et al.*, 1980). Monteiro *et al.* (2013) have reported that TG degree of branching is 2.83 ± 0.07 and that its average molecular weight is (2.09 ± 0.05) x 10^6. TG disperses and hydrates in cold or hot water, and form very viscous solutions. Due to these characteristics, it can be used by the food industry as a stabilizing agent, emulsifier and thickener, and to avoid undesirable effects in gelled products like syneresis. Some authors have reported that the presence of TG improves the functional properties of other hydrocolloids such as κ-carrageenan, agar, and xanthan gum, demonstrating a marked synergistic effect (Daas *et al.* 2002). Given these functional properties, many scientists are increasingly beginning to pay more attention to technological exploitation of TG in various fields (Antoniou *et al.* 2015).

Bovine sodium caseinate (NaCAS) is a protein derivative widely used in dairy, bakery, and meat industries because of its high nutritional value and specific functionalities such as emulsifying, foaming, gelling, and texture improving properties (Sadeghi *et al.* 2018).

Acid gelation of proteins is an important unit operation in the development and manufacture of acid dairy foods, such as yoghurt-like desserts, soft cheeses, and tofu-type products (Gu *et al.* 2009; Picone and da Cunha 2010; Kumar *et al.* 2019). The glucono-δ-lactone (GDL) induces acid gelation because it contains an internal ester that, in aqueous solution, hydrolyses to form gluconic acid (de Kruif 1997). The use of GDL as acidulant enables different rates of acidification, depending on the GDL concentration, the temperature, and the presence of polysaccharides (Braga and Cunha 2004). Also, since GDL-

induced gel obtainment can involve lower temperatures than those implied in heat-induced gelation, these acid gels can be considered as a device for encapsulation and protection of heat-sensitive bioactive compounds (Chen *et al.* 2019).

Bovine sodium caseinate acid gelation has already been reported in the presence of a wide variety of others galactomannans, like locust bean, guar, and espina corona gums (Perrechil *et al.* 2009; Hidalgo *et al.* 2015; López *et al.* 2017a). On the other hand, some authors have reported the interaction of β-lactoglobulin and TG and the whey protein isolates/TG mixed gels obtention (Tavares *et al.* 2005; Sittikijyothin *et al.* 2010). However, the interaction between TG and NaCAS, and the effect of this hydrocolloid on the NaCAS acid gelation has not yet been elucidated.

The aim of this work was to evaluate the microstructural, rheological, and textural behaviour of TG-NaCAS aqueous mixtures and their acid gels. The present findings might have important implications not only for the development of new food grade gels with different textures but also for the obtention of stable W/W emulsions, and thus, the opening a wide range of novel possibilities for practical applications such as the delivery of bioactive compounds.

MATERIALS AND METHODS

Materials

Bovine sodium caseinate powder (NaCAS) and glucono-δ-lactone (GDL) were purchased from Sigma-Aldrich Co. (Steinheim, Germany), and used without further purification. The casein composition of NaCAS was 45, 12, 33, and 10 g/100 g for α_{S1}-, α_{S2}-, β-, and κ-casein fractions, respectively. Tara gum (TG) was of food-grade and provided by G y G Suministros

(Rosario, Argentina). Rhodamine B was of analytical grade and provided by Ciccarelli SRL (San Lorenzo, Argentina).

Methods

Sample preparation

Tara gum and NaCAS aqueous stock solutions (2.0 g/100 g and 8.0 g/100 g, respectively) were prepared from the dissolution of powders in distilled water under magnetic stirring at room temperature and storage at 4 °C.

Binary solutions of TG-NaCAS were prepared by mixing weighed amounts of TG and NaCAS aqueous stock solutions and additional distilled water (when it was necessary) at room temperature.

For thermodynamic compatibility assays, NaCAS and TG solutions were prepared in 10 mM Tris-HCl buffer pH 6.80.

Phase diagram

Binary systems were prepared keeping, in one case, the same TG concentration (C_{TG}) but with NaCAS concentrations (C_{NaCAS}) ranging from 0.5 to 3.0 g/100 g and, in the other case, the same C_{NaCAS} but with C_{TG} ranging from 0.1 to 0.8 g/100 g. The systems were mixed and incubated for 48 h at three different temperatures (4, 18, and 36 °C). The segregative phase separation that occurs between a galactomannan and a charged protein may not be observed immediately because of the particular characteristics of the kinetic process (Bryant and McClements 2000). Therefore, at greater times, macroscopic phase separation may be observed (Stieger and van de Velde 2013). After incubation times, the appearance of turbidity

and/or separation of phases was analysed by visual inspection as was proposed by Spyropoulos, Portsch, & Norton (2010).

Zeta potential measurement

Zeta potential (ζ) of NaCAS and TG aqueous solution was determined at 25°C in a Nano Particle Analyzer Horiba SZ-100 (HORIBA, Kyoto, Japan). C_{NaCAS} was fixed at 3.0 g/100 g whereas C_{TG} varied over the range of 0 - 0.5 g/100 g. The distilled water used to prepare the dispersions was filtered through a Minisart® Syringe filter (Sartorius Stedim Biotech GmbH, Goellingen, Germany) with a cut-off of 0.2 μm in order to avoid powders in suspensions, that could interferences with the technique (Anema and Klostermeyer 1996).

Fourier transform infrared (FTIR) spectroscopy of TG

To obtain FTIR spectra, solid samples of TG were previously dispersed in distilled water at 1.0 g/100 g. Each dispersion (100 μL) was put in the ZnSe ATR device, covering the entire crystal and then was gently dried with warm air until total dehydration. All FTIR spectra were obtained at room temperature with a Shimadzu model IR Affinity-1 device (Shimadzu Corporation; Kyoto, Japan) under the following conditions: Happ-Genzel Appodization; number of scans: 25, Resolution: 4 cm^{-1}; wavenumber range: 650 to 4000 cm^{-1}.

Binary system acid gelation

Binary systems were prepared keeping constant the C_{NaCAS} (3.0 g/100 g) whereas C_{TG} varied over the range of 0-0.5 g/100 g. The amount of GDL added was calculated using the following relation (R):

$$R = \frac{\text{GDL mass fraction}}{\text{NaCAS mass fraction}} \quad (1)$$

Binary system acid gelation was initiated by the addition of solid GDL according to R = 0.5 at 18 °C.

Oscillatory dynamic rheology assays

Rheological characteristics of NaCAS (3.0 g/100 g) gelling behaviour, in the absence or presence of TG (CTG 0.05, 0.10, 0.20, 0.30, and 0.50 g/100 g), were determined in a stress and strain-controlled AR G2 model rheometer (TA Instruments Waters LLC; New Castle, DE, USA) using a cone geometry (diameter: 40 mm, cone angle: 2°, cone truncation: 55 mm). Temperature was set at 18 °C through a system of temperature control with a recirculating bath (Julabo model ACW100, Germany) connected to a Peltier plate. An adequate amount of GDL (R = 0.5) was added to initiate the acid gelation and time sweep steps were performed at an oscillation stress of 0.1 Pa and a frequency of 0.1 Hz. The Lissajous figures at various times were plotted to ensure that the measurements of storage or elastic modulus (G') and loss or viscous modulus (G'') were always obtained within the linear viscoelastic region.

The G'- G'' crossover times (t_{gel}) of acidified systems were considered as the gel times. The pH at t_{gel} was also determined considering the pH value at the G'-G'' crossover (pH_{gel}). Also, the maximum storage modulus (G'_{max}) was determined. Once the system reached the equilibrium, a frequency sweep step was performed in the range of 0.1–10 Hz frequency in

161 the field of linear viscoelasticity at 18°C. The frequency dependence of G' was quantified
162 for each acid gel by fitting the power law equation:

163 $$G' = K'\omega^{n'} \quad (2)$$

164 where ω, K', and n' are the angular frequency, the power law constant and the frequency
165 exponent, respectively (Bi *et al.* 2013).

166

167 **Confocal scanning laser microscopy (CSLM) assays**

168 Bovine sodium caseinate (C_{NaCAS} = 3.0 g/100 g) without and with TG (C_{TG} = 0.10; 0.20;
169 0.30, 0.40, and 0.50 g/100 g) were stained with Rhodamine B solution (final concentration 2
170 mg/L). An adequate amount of GDL (R = 0.5) was added to initiate the acid gelation process
171 at 18 °C. Aliquots of 200 μL were immediately placed in compartments of LAB-TEK II cells
172 (Thermo Scientific, USA). Gels were observed with a 20× objective, with 4× zoom, by using
173 an inverted scan confocal microscope NIKON Eclipse TE-2000-E (Nikon Instruments Inc.,
174 Japan), with handheld scanning, using 543 nm excitation He-Ne laser, 605-675 nm band
175 emission. Acquired images were stored in tiff format for their further analysis.
176 On the other hand, to observe the kinetics of the segregative phase separation process of TG-
177 NaCAS mixtures (C_{NaCAS} 3.0 g/100 g and C_{TG} 0.30 g/100 g), CLSM images were obtained
178 in the same conditions described above, immediately after mixing NaCAS and TG, in the
179 absence of GDL.

180

181 **Environmental scanning electron microscopy (ESEM) assays**

182 Liquid samples of a TG-NaCAS GDL-acidified system (C_{NaCAS} 3.0 g/100 g, C_{TG} 0.2 g/100
183 g, R = 0.50) were placed on aluminium stubs using double-sided carbon adhesive tape, and

observed directly under an electron microscope (Zeiss, Evo LS10, Germany) at 15 kV, using a backscattered detector at 30 Pa vapor pressure. ESEM images were obtained at 1000× and 2000× magnification and stored at a resolution of 2048 x 1536 pixels in TIFF format.

Textural assays

To evaluate the effect of C_{TG} in the textural characteristics of TG-NaCAS acid gels, a texture profile analysis (TPA) was carried out at room temperature with a Perten TVT 6700 Texture Analyzer (Perten Instruments, Hägersten, Sweden) using a cylindrical probe (diameter = 25 mm). Mixed acid gels (C_{NaCAS} 3.0 g/100 g, R = 0.5, and C_{TG} 0, 0.05, and 0.10 g/100 g) were prepared in cylindrical containers (45 mm diameter and 30 mm height) and were incubated at 18 °C for 90 min.

Each sample (cylinders of 17 mm height) was penetrated axially in a single cycle of 50 % of compression at a constant speed of 1.0 mm/s. From the TPA curves, the following texture parameters were obtained: firmness (FI, N/mm), defined as the initial slope of the penetration profiles obtained, and fracture force (FF, N), defined as the force at the first significant gel break.

Water holding capacity (WHC)

Water holding capacity (WHC) was determined by using the method described by Pang *et al*. (2015). Acid gel samples (15 g) of NaCAS (C_{NaCAS} = 3.0 g/100 g) in the absence or in the presence of different C_{TG} (0.05, 0.10, 0.15, and 0.20 g/100 g) were prepared in plastic tubes by GDL addition (R=0.5) and after incubation at 18 °C for 90 min. The final pH of all these acid gels was 4.17 ± 0.04. These tubes were weighed and then centrifuged at 200 x g for 15

min. Serum expelled was then weighed and the WHC, expressed as a percentage, was calculated using the equation (3):

$$WHC\ (\%) = 100 * \left[\frac{(\text{gel weight} - \text{serum weight})}{\text{gel weight}} \right] \quad (3)$$

Statistical analysis

Data presented are the average values ± standard deviations. The statistical analysis was performed by analysis of variance (ANOVA) and Tukey test with Sigma Plot software (10.0 trial version). The relationship between variables was evaluated by correlation analysis, using the Pearson correlation coefficient (p). Differences were considered statistically significant at $p < 0.05$ values.

RESULTS AND DISCUSSION

Zeta potential (ζ) of TG-NaCAS mixtures

Table 1 shows the ζ determined in the NaCAS, TG, and TG-NaCAS mixtures.

It was observed that as C_{TG} increases, ζ of TG-NaCAS mixtures decreases. This fact may be associated with changes in the balance between exposed hydrophobic/hydrophilic groups as was reported by Picullel and Lindman (1992).

On the other hand, ζ of TG aqueous solutions was determined at different C_{TG} (0.10, 0.30, and 0.50 g/100 g). No significant differences were found among these dispersions, showing a negative ζ of (-19.8 ± 0.7) mV. This value was slightly higher to that reported by Carnero-da-Cunha *et al*. (2011) for a *Gleditsia triacanthos* galactomannan (*Gtg*). In this case, these authors indicate that a ζ of -13.0 mV for *Gtg* aqueous solution (2 g/L) confirm a neutral

behaviour. However, in the same report, these authors also observed that hydrodynamic diameter (Z-average) of *Gtg* aqueous solutions was significantly affected by pH, indicating an electrostatic repulsion of molecules, which is in contradiction to their previous conclusion. In a more recent study, Haddarah *et al*. (2014) also reported negative ζ for another galactomannan, ranging from -2.67 to -12.95 mV according to the legume variety and geographical localization. In this context, the fact that ζ values of TG-NaCAS mixtures decreased as C_{TG} increases (Table 1), while TG and NaCAS solutions have negative ζ values, could imply the existence of conformational changes probably due to the exclusion of TG colloidal particles from the protein surface. This behaviour was also reported by Ingrassia *et al*. (2019a) for TG-soy protein isolate cold-set gels. This decrease in the surface charge of NaCAS particles could weaken the inter-particle electrostatic repulsion, promoting the protein aggregation. Thus, this formation of protein aggregates implies a structural change that promote a lower exposure of NaCAS acidic residues. This phenomenon should be considered in order to evaluate the gelling behaviour of NaCAS in TG-NaCAS mixtures.

FTIR spectroscopy

Because the TG solutions, a neutral galactomannan, showed negative ζ values ((-19.8 ± 0.7) mV), FTIR spectra were carried out to analyse the TG samples. It is known that proteins may be present as contaminants in food-grade galactomannans since they may come from the remaining germ or seed coat traces in the extracted gum (Liyanage *et al.* 2015). In this context, Liyanage *et al*. (2015) used FTIR spectroscopy as a fast and non-destructive analytical tool for the identification of possible contaminants present in guar galactomannan samples. In the same way, in order to confirm the presence of proteins in TG sample, which

253 may hence be responsible for providing sample negative charge observed by ζ
254 determinations, FTIR spectrum of TG was obtained and is shown in Figure 1.
255 Tara gum spectrum shows the typical galactomannan peaks at 812 and 871 cm^{-1} in the
256 fingerprint region (900-700 cm^{-1}), which are related with the presence of α-linked D-
257 galactopyranose units and β-linked D-mannopyranose units, respectively. Also, TG shows
258 the typical broad-band between 1200 and 900 cm^{-1}, known as the carbohydrate region, which
259 is related to stretching vibration of C–O in C–O–H bonds (e.g. glycosidic bonds) and is
260 related with the galactomannans' sugar composition. The peak at 1152 cm^{-1} is assigned to
261 bending vibrational modes of C-O of the pyranose ring, whereas peaks detected between
262 1134 and 983 cm^{-1} regions (centred at 1063.5 and 1025 cm^{-1}) are assigned to C-OH bending.
263 TG spectrum also shows a band at 1640 cm^{-1}, which is attributed to adsorbed water
264 (Cerqueira *et al.* 2011). According to Liyanage *et al*. (2015), the presence of proteins are
265 revealed as additional bands at 1543 and 1740 cm^{-1}, which are related to C=O stretching and
266 NH_2 deformation. As Figure 1 shows, there would be no significant protein contamination in
267 TG samples.
268
269 **Thermodynamic incompatibility of TG-NaCAS mixtures**
270 Figure 2 shows an approach used for the determination of the phase diagrams for TG-NaCAS
271 binary systems incubated at different temperatures after 48 h.
272 At all the temperatures assayed, macroscopic phase separation areas were observed.
273 According to the ζ values of TG-NaCAS mixtures previously reported, the behaviour
274 observed was a segregative phase separation. Similar results were reported for xantham gum-
275 whey protein mixtures (Bryant and McClements 2000), β-lactoglobuline-TG binary systems
276 (Sittikijyothin *et al.* 2010), guar gum-NaCAS mixtures (Hidalgo *et al.* 2015), and espina

277 corona gum-NaCAS mixed systems (López *et al.* 2017b). In all the cases, it was observed a
278 lower protein-rich phase and an upper polysaccharide-rich phase.
279 In addition, Figure 3 shows the CLSM images of TG-NaCAS mixture at different times. It
280 can be observed, along the time, the protein aggregate formation in red colour, while dark
281 areas correspond to the polysaccharide-rich phase. After mixing NaCAS and TG, it can be
282 observed a protein aggregation process over time that leads to segregative phase separation.
283 This phase separation may occur because of the existence of NaCAS-TG depletion
284 interaction, linked to the repulsion between both polymeric systems at a critical NaCAS and
285 TG concentration. At high protein concentrations, when the NaCAS particles approach and
286 their depletion layers overlap, the volume of the available solution for TG increases. This
287 generates an increase in the entropy and the consequent decrease in the free energy, which
288 causes an attractive interaction between protein particles. Other authors have reported that
289 protein-polysaccharide incompatibility takes place impelled by depletion forces (Tuinier *et*
290 *al.* 2000; Rediguieri *et al.* 2007).
291 Moreover, as temperature increases, the areas where segregative phase separation occurs,
292 increase (Figure 2). This behaviour is due to the delay of phase separation because of the
293 restricted movement of the highly viscous biopolymers solutions. Hence, as the temperature
294 increases, binary solutions viscosity for the same biopolymer concentrations decreases, and
295 the number of protein-protein interactions increases. As a result, the biopolymer
296 concentrations from which segregative phase separation occurs, decrease.
297

298 **Rheological analysis of TG-NaCAS acid gels**

299 All the samples assayed (C_{NaCAS} 3.0 g/100 g and C_{TG} 0, 0.05, 0.10, 0.20, 0.30, and 0.50 g/100
300 g) formed acid gels after GDL addition (R = 0.50) at 18 °C and showed a viscoelastic

evolution upon acidification. As an example, Figure 4 A shows G' and G'' as a function of time of NaCAS sample (3.0 g/100 g) during acid gelation. At initial times, both moduli remained in small values and the sample showed a liquid-like behaviour, since G' is lower than G''. After some time, G' and G'' increase and reach a plateau value, where G' is higher than G'', indicating a solid-like behaviour. This behaviour upon GDL-acidification also has been reported by several authors in previous works (Hidalgo *et al.* 2015; Ingrassia *et al.* 2019b; Mession *et al.* 2015; Alting *et al.* 2003). Besides, in order to elucidate the physical structure of the acid gels obtained, a frequency sweep step was performed when the system reached the equilibrium. Figure 4 B shows G' and G'' behaviour (both moduli increase) upon frequency changes (0.1–10 Hz) of NaCAS gelled system. NaCAS and TG-NaCAS binary systems showed n' > 0 (data not shown), indicating the physical nature of the acid gels (Stading and Hermansson 1990). These n' values showed no significant differences among samples ($p > 0.05$) ranging from 0.177 to 0.236, indicating a same frequency dependence of G', that is, the gel structure is not affected by the change in frequency. Ingrassia *et al.* reported a similarly behaviour for cold-set gels of defatted soy flour (Ingrassia *et al.* 2019b).

Table 2 shows t_{gel}, pH_{gel}, and G'_{max} values obtained for NaCAS and TG-NaCAS acid gels. Prior to discussing these results, it is important to notice that the presence of TG did not affect GDL hydrolysis because the pH acidification rate did not change in NaCAS and TG-NaCAS GDL-acidified systems (data not shown).

It is known that to achieve protein acid gelation the removal of electrostatic repulsion due to the negative ζ of NaCAS particles is required. This can be achieved by the binding of protons during the acid gelation process. However, although NaCAS particles presented a significant decrease in the surface charge with TG concentration (Table 1), pH_{gel} values (Table 2)

showed no significant differences among samples ($p > 0.05$). Therefore, this result implies that the same amount of H^+ is needed to achieve NaCAS gelation in all samples.

The t_{gel} values showed no significant differences among samples, except for TG-NaCAS mixed system containing 0.5% of TG, where the t_{gel} decreases significantly ($p < 0.05$). According to Table 1, the negative ζ is the lowest at this C_{TG}. Thus, TG-NaCAS samples with highest C_{TG} are more electrostatically unstable and, as a consequence, the t_{gel} decreases. Also, and due to the segregative phase separation observed at high C_{TG} (Figure 2), initial protein aggregates would exist in this TG-NaCAS mixture. Therefore, t_{gel} value may tend to be lower than t_{gel} in the corresponded TG-NaCAS mixture without these initial protein aggregates.

On the other hand, G'_{max} values decrease with C_{TG}, revealing an elastic behavior loss in the presence of higher amounts of TG. As mentioned above, at higher concentrations of TG, phase separation due to thermodynamic incompatibility occurs, competing with the gelation process and promoting the formation of weaker gels.

TG-NaCAS acid gels microstructure

Figure 5 shows the digital images obtained by CSLM of NaCAS acid gels (C_{NaCAS} = 3.0 g/100 g) in the absence and the presence of different C_{TG} (0.05, 0.10, 0.20, 0.30, and 0.50 g/100 g), after addition of GDL (R 0.5 and 18 ºC).

In the absence (Figure 5 A) and the presence of C_{TG} 0.05 and 0.10 g/100 g (Figure 5 B and C, respectively), it was observed a continuous protein gel matrix where dark zones represent the gel mesh pores and the red ones the NaCAS network. Also, it can be observed that the

346 pore size of the gel network increase with C_{TG}, i.e., the compactness degree of gel mesh
347 decrease.
348 On the other hand, in the presence of C_{TG} 0.20, 0.30, and 0.50 g/100 g (Figure 5 D, E, and F,
349 respectively), protein droplet-shaped structures were observed. In this case, the protein phase
350 is compressed into spheres with an average diameter of 2-4 μm. Therefore, at these higher
351 C_{TG} ($C_{TG} \geq 0.2$ g/100 g), the mixed TG-NaCAS gel microstructure was modified from a
352 protein continuous network to protein droplet-shaped structures. Figure 6 shows the digital
353 images obtained by ESEM obtained at 1000× (Figure 6 A) and 2000× (Figure 6 B), also
354 revealing the droplet-shaped structure of these microparticles. Also, it is important to
355 highlight that the average diameter of these particles is in good correlation with those
356 obtained by CSLM.
357 At high concentrations of both types of macromolecules, repulsive interactions between both
358 biopolymers promote segregative phase separation. At a constant NaCAS concentration, the
359 TG rich-phase volume fraction increases with TG concentration. As a consequence, the
360 NaCAS rich-phase volume fraction decreases and this induces protein self-association in
361 protein droplet-shaped structures. In addition, the decrease in the electrostatically stability of
362 NaCAS particles when C_{TG} increases (Table 1), may also promote this behaviour. Moreover,
363 at lower acidification rates, when acid protein gelation and phase separation processes
364 simultaneously occur, phase separation prevails on the gel formation due to slower gelation
365 kinetics (Stieger and van de Velde 2013). Hence, these protein droplet-shaped structures are
366 W/W emulsions of NaCAS droplets in a TG aqueous continuous phase, stabilized by protein
367 gelation that prevents drop coalescence. The formation of this type of microstructure,

368 presenting no interconnected gel mesh, is consistent with the decrease in the elastic character
369 of the gels.
370 Esquena (2016) has defined W/W emulsion as droplets of an aqueous phase dispersed into
371 another aqueous phase formed in mixtures of at least two water-soluble molecules, which are
372 mutually incompatible in solution. These W/W emulsions are unstable due to the absence of
373 repulsive forces between the droplets. Capron *et al*. (2001) studied a ternary system
374 composed by NaCAS and alginate in aqueous solution and they postulated the importance of
375 the interface mobility on the W/W emulsion stability. Lundin *et al*. (1999) succeeded in the
376 obtention of stable W/W emulsions by controlling the thermal gelation rate in aqueous
377 mixtures of gelatin and ι-carrageenan due to the formation of gelled states that prevent
378 coalescence. In the present work, we have observed W/W emulsions of TG-NaCAS aqueous
379 system stabilized by acid gelation. In agreement with the proposal enunciated by Esquena
380 (2016), these W/W emulsions stabilized by acid gelation gives rise to the formation of
381 colloidal dispersions of microgel particles.
382 Similarly, Hidalgo *et al*. (2015) also informed the dependence of NaCAS acid-induced gel
383 microstructure on guar gum concentration, another galactomannan with similar
384 characteristics to TG. They also reported the formation of NaCAS-droplet-shaped structures
385 at the same NaCAS concentration but at higher polysaccharide concentrations.
386 As above mentioned, during the acidification process, the protein gelation and the segregative
387 phase separation simultaneously occurs. If the protein gelation rate is higher than segregative
388 phase separation, it is possible the formation of an interconnected gel mesh (Figure 5 B and
389 C). However, at $C_{TG} \geq 0.20$ g/100 g, when the segregative phase separation is the

predominant process, stable-W/W emulsions are generated. This latter phenomenon results in a weak gel formation without a continuous protein three-dimensional network.

Taking into account what it was observed in Figure 3 (in the absence of GDL) and in Figure 5 E (in the presence of GDL), where the concentrations of both biopolymers are the same (C_{NaCAS} 3.0 g/100 g and C_{TG} 0.3 g/100 g), it can be concluded the obtainment of stable W/W emulsions is achieved through the generation of gelled states, and thus avoiding coalescence.

Textural assays

Table 3 shows the values of FI and FF obtained in the absence and in the presence of $C_{TG} \leq$ 0.10 g/100 g. It is important to clarify that in systems with $C_{TG} \geq 0.20$ g/100 g, associated texture parameters could not be obtained due to the critical weakness of the gels checked by G'_{max} parameter decrease.

No significant differences were observed in the FF values obtained. On the other hand, the presence of TG in TG-NaCAS mixtures at a concentration that allows the formation of a continuous protein gel network (Figure 5 A-C) promote a significant FI decrease. This behaviour is related to the increase in the pore size of NaCAS gel network described above.

Water holding capacity (WHC)

Table 4 shows the WHC of TG-NaCAS acid gels obtained in the absence of TG and in the presence of different C_{TG} (0.05-0.20 g/100 g).

When C_{TG} was $\leq$ 0.10 g/100 g, NaCAS acid-gels did not show significant changes in WHC. On the other hand, when C_{TG} was $\geq$ 0.15 g/100 g, the WHC of the acid-gels abruptly decreased. These results can be related to the type of gel microstructure obtained. In the first case, when the microstructure corresponds to a continuous and interconnected gel network,

414 the WHC is not significantly affected, since the serum is trapped in the gel mesh. When the
415 formation of W/W emulsions stabilized by gelation are observed, this network
416 interconnection is lost, and with it, the capability to retain water.
417
418 ## CONCLUSIONS
419 Depending on the TG concentration, TG-NaCAS acid gels with different microstructures,
420 rheological behaviour, and water holding capacities were obtained. These results are linked
421 with a competition between the protein acid gelation process and the segregative phase
422 separation. Depending on the concentration ratio of both biopolymers, a continuous protein
423 gel network (0 - 0.10 g/100 g of TG) or W/W emulsions stabilized by acid gelation (stable
424 W/W emulsions) were observed (0.2-0.5 g/100 g of TG).
425 These findings may be used not only to develop new food grade gels with different textures
426 but also for the obtention of NaCAS microgels to encapsulate hydrophilic compounds. In this
427 sense, we consider that it would be necessary to deepen the study of other conditions to which
428 W/W emulsions are obtained from mixtures of TG and NaCAS.
429
430 ## ACKNOWLEDGMENT
431 The authors would like to thank the staff from the English Department (Facultad de Ciencias
432 Bioquímicas y Farmacéuticas, UNR) for the language correction of the manuscript, and to
433 Universidad Nacional de Rosario (UNR) who provided the financial support (1BIO439).
434
435 ## REFERENCES

436 Alting A C, Hamer R J, De Kruif C G and Visschers R W (2003) Cold-Set Globular Protein
437 Gels: Interactions, Structure and Rheology as a Function of Protein Concentration. *Journal*
438 *of Agricultural and Food Chemistry* **51** 3150-3156.
439 Anema S G and Klostermeyer H (1996) ζ-Potentials of casein micelles from reconstituted
440 skim milk heated at 120 °C. *International Dairy Journal* **6** 673-687.
441 Antoniou J, Liu F, Majeed H and Zhong F (2015) Characterization of tara gum edible films
442 incorporated with bulk chitosan and chitosan nanoparticles: A comparative study. *Food*
443 *Hydrocolloids* **44** 309-319.
444 Bi C H, Li D, Wang L J, Wang Y and Adhikari B (2013) Characterization of non-linear
445 rheological behavior of SPI–FG dispersions using LAOS tests and FT rheology.
446 *Carbohydrate Polymers* **92** 1151-1158.
447 Braga A L M and Cunha R L (2004) The effects of xanthan conformation and sucrose
448 concentration on the rheological properties of acidified sodium caseinate-xanthan gels. *Food*
449 *Hydrocolloids* **18** 977-986.
450 Bryant C M and McClements D J (2000) Influence of xanthan gum on physical
451 characteristics of heat-denatured whey protein solutions and gels. *Food Hydrocolloids* **14**
452 383-390.
453 Buffington L A, Stevens E S, Morris E R and Rees D A (1980) Vacuum ultraviolet circular
454 dichroism of galactomannans. *International Journal of Biological Macromolecules* **2** 199-
455 203.
456 Capron I, Costeux S and Djabourov M (2001) Water in water emulsions: phase separation
457 and rheology of biopolymer solutions. *Rheologica Acta* **40** 441-456.
458 Carneiro-Da-Cunha M G, Cerqueira M A, Souza B W S, Teixeira J A and Vicente A A (2011)
459 Influence of concentration, ionic strength and pH on zeta potential and mean hydrodynamic

460 diameter of edible polysaccharide solutions envisaged for multinanolayered films
461 production. *Carbohydrate Polymers* **85** 522-528.
462 Cerqueira M A, Bourbon A I, Pinheiro A C, Martins J T, Souza B W S, Teixeira J A and
463 Vicente A A (2011) Galactomannans use in the development of edible films/coatings for
464 food applications. *Trends in Food Science & Technology* **22** 662-671.
465 Corredig M, Sharafbafi N and Kristo E (2011) Polysaccharide–protein interactions in dairy
466 matrices, control and design of structures. *Food Hydrocolloids* **25** 1833-1841.
467 Chen X M, Yuan J L, Li R X and Kang X (2019) Characterization and embedding potential
468 of bovine serum albumin cold-set gel induced by glucono-δ-lactone and sodium chloride.
469 *Food Hydrocolloids* **95** 273-282.
470 Daas P, Grolle K, Van Vliet T, Schols H and De Jongh H (2002) Toward the Recognition of
471 Structure-Function Relationships in Galactomannans. *Journal of Agriculture and Food*
472 *Chemistry* **50** 4282-4289.
473 De Kruif C G (1997) Skim Milk Acidification. *Journal of Colloid and Interface Science* **185**
474 19-25.
475 Esquena J (2016) Water-in-water (W/W) emulsions. *Current Opinion in Colloid & Interface*
476 *Science* **25** 109-119.
477 Ghosh A K and Bandyopadhyay P (2012) Polysaccharide-Protein Interactions and Their
478 Relevance in Food Colloids. In: *The Complex World of Polysaccharides*, pp. Ch. 14.
479 KARUNARATNE, D N ed. Rijeka: InTech.
480 Gu X, Campbell L J and Euston S R (2009) Influence of sugars on the characteristics of
481 glucono-[delta]-lactone-induced soy protein isolate gels. *Food Hydrocolloids* **23** 314-326.

Haddarah A, Bassal A, Ismail A, Gaiani C, Ioannou I, Charbonnel C, Hamieh T and Ghoul M (2014) The structural characteristics and rheological properties of Lebanese locust bean gum. *Journal of Food Engineering* **120** 204-214.

Hidalgo M E, Fontana M, Armendariz M, Riquelme B, Wagner J and Risso P (2015) Acid-Induced Aggregation and Gelation of Sodium Caseinate-Guar Gum Mixtures. *Food Biophysics* **10** 181-194.

Ingrassia R, Bea L L, Hidalgo M E and Risso P H (2019a) Microstructural and textural characteristics of soy protein isolate and tara gum cold-set gels. *LWT* **113** In press.

Ingrassia R, Palazolo G G, Wagner J R and Risso P H (2019b) Heat treatments of defatted soy flour: Impact on protein structure, aggregation, and cold-set gelation properties. *Food Structure* **22** 100-130.

Kumar R, Mishra D, Sutariya H, Chaudhary M B and Rao K J (2019) Effect of different coagulants on the yield, sensory, instrumental colour and textural characteristics of cow's milk Paneer. *International Journal of Dairy Technology* **72** 617-625.

Liyanage S, Abidi N, Auld D and Moussa H (2015) Chemical and physical characterization of galactomannan extracted from guar cultivars (*Cyamopsis tetragonolobus* L.). *Industrial Crops and Products* **74** 388-396.

López D N, Galante M, Alvarez E M, Risso P H and Boeris V (2017a) Effect of the espina corona gum on caseinate acid-induced gels. *LWT - Food Science and Technology* **85, Part A** 121-128.

López D N, Galante M, Alvarez E M, Risso P H and Boeris V (2017b) Physicochemical study of mixed systems composed by bovine caseinate and the galactomannan from Gleditsia amorphoides. *Carbohydrate Polymers* **173** 1-6.

505 Lundin L, Norton I, Foster T, Williams M, Hermansson A and Bergström E (1999) Phase
506 separation in mixed biopolymer systems. In: *10th International gums and stabilizers for the*
507 *food industry: the past, present and future of food hydrocolloids,* pp. 167–180. WILLIAMS,
508 P and PHILLIPS, G eds. Cambridge, UK: Woodhead Publishing
509 Mession J L, Chihi M L, Sok N and Saurel R (2015) Effect of globular pea proteins
510 fractionation on their heat-induced aggregation and acid cold-set gelation. *Food*
511 *Hydrocolloids* **46** 233-243.
512 Monteiro S R, Rebelo S, Da Cruz e Silva O A B and Lopes-Da-Silva J A (2013) The influence
513 of galactomannans with different amount of galactose side chains on the gelation of soy
514 proteins at neutral pH. *Food Hydrocolloids* **33** 349-360.
515 Norton I T and Frith W J (2001) Microstructure design in mixed biopolymer composites.
516 *Food Hydrocolloids* **15** 543-553.
517 Pang Z, Deeth H, Sharma R and Bansal N (2015) Effect of addition of gelatin on the
518 rheological and microstructural properties of acid milk protein gels. *Food Hydrocolloids* **43**
519 340-351.
520 Perrechil F A, Braga A L M and Cunha R L (2009) Interactions between sodium caseinate
521 and LBG in acidified systems: Rheology and phase behavior. *Food Hydrocolloids* **23** 2085-
522 2093.
523 Picone C S F and Da Cunha R L (2010) Interactions between milk proteins and gellan gum
524 in acidified gels. *Food Hydrocolloids* **24** 502-511.
525 Piculell L and Lindman B (1992) Association and segregation in aqueous polymer/polymer,
526 polymer/surfactant, and surfactant/surfactant mixtures: similarities and differences.
527 *Advances in Colloid and Interface Science* **41** 149-178.

Rediguieri C F, De Freitas O, Lettinga M P and Tuinier R (2007) Thermodynamic Incompatibility and Complex Formation in Pectin/Caseinate Mixtures. *Biomacromolecules* **8** 3345-3354.

Sadeghi F, Kadkhodaee R, Emadzadeh B and Phillips G O (2018) Phase behavior, rheological characteristics and microstructure of sodium caseinate-Persian gum system. *Carbohydrate Polymers* **179** 71-78.

Sittikijyothin W, Sampaio P and Gonçalves M P (2010) Microstructure and rheology of β-lactoglobulin–galactomannan aqueous mixtures. *Food Hydrocolloids* **24** 726-734.

Spyropoulos F, Portsch A and Norton I T (2010) Effect of sucrose on the phase and flow behaviour of polysaccharide/protein aqueous two-phase systems. *Food Hydrocolloids* **24** 217–226.

Stading M and Hermansson A M (1990) Viscoelastic behaviour of β-lactoglobulin gel structures. *Food Hydrocolloids* **4** 121-135.

Stieger M and Van De Velde F (2013) Microstructure, texture and oral processing: New ways to reduce sugar and salt in foods. *Current Opinion in Colloid & Interface Science* **18** 334-348.

Tavares C, Monteiro S R, Moreno N and Lopes Da Silva J A (2005) Does the branching degree of galactomannans influence their effect on whey protein gelation? *Colloids and Surfaces A: Physicochemical and Engineering Aspects* **270–271** 213-219.

Tolstoguzov V B (1991) Functional properties of food proteins and role of protein-polysaccharide interaction. *Food Hydrocolloids* **4** 429-468.

Tuinier R, Dhont J K G and De Kruif C G (2000) Depletion-Induced Phase Separation of Aggregated Whey Protein Colloids by an Exocellular Polysaccharide. *Langmuir* **16** 1497-1507.

Figure 1

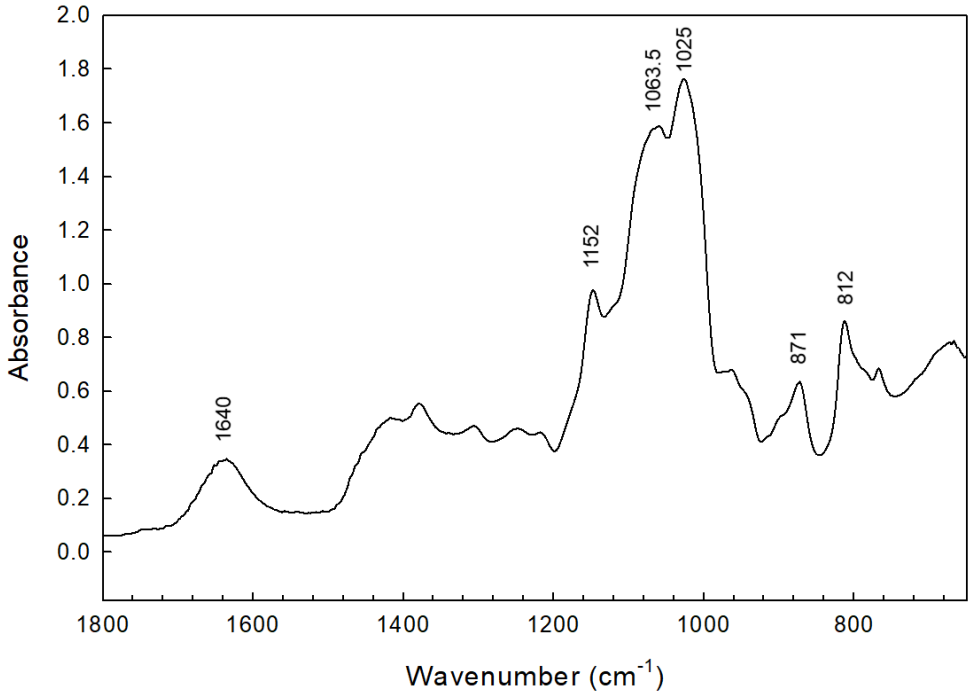
Absorbance
Wavenumber (cm-1)
1640
1152
1063.5
1025
871
812
2.0
1.8
1.6
1.4
1.2
1.0
0.8
0.6
0.4
0.2
0.0
1800
1600
1400
1200
1000
800

Figure 2

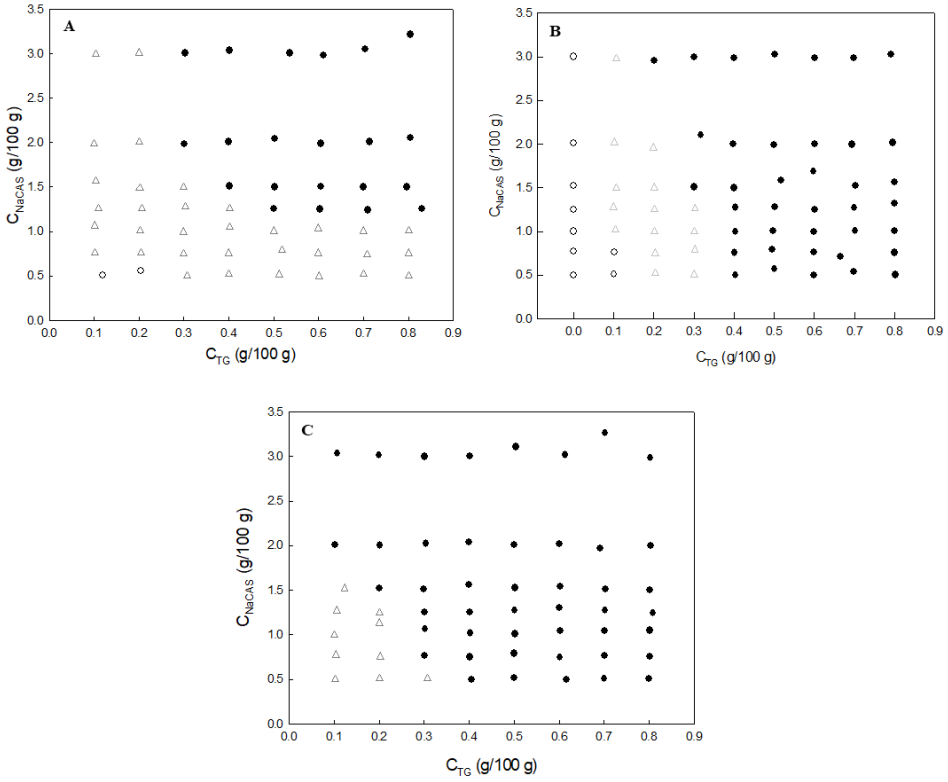

Figure 3

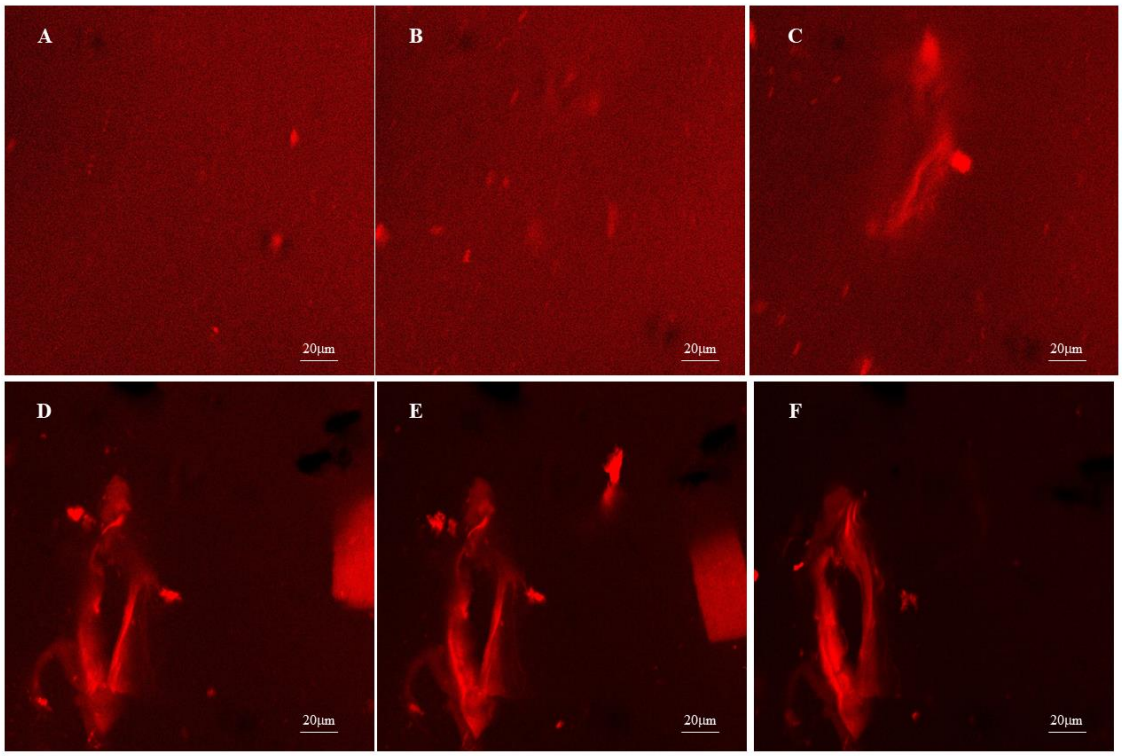

Figure 4

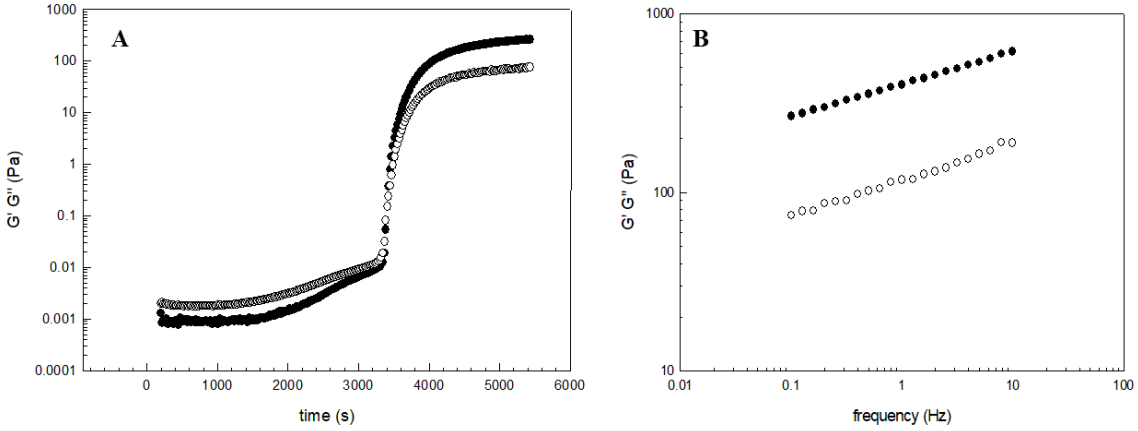
A
B
G' G'' (Pa)
time (s)
frequency (Hz)
1000
100
10
1
0.1
0.01
0.001
0.0001
0
1000
2000
3000
4000
5000
6000
0.01
0.1
1
10
100

Figure 5

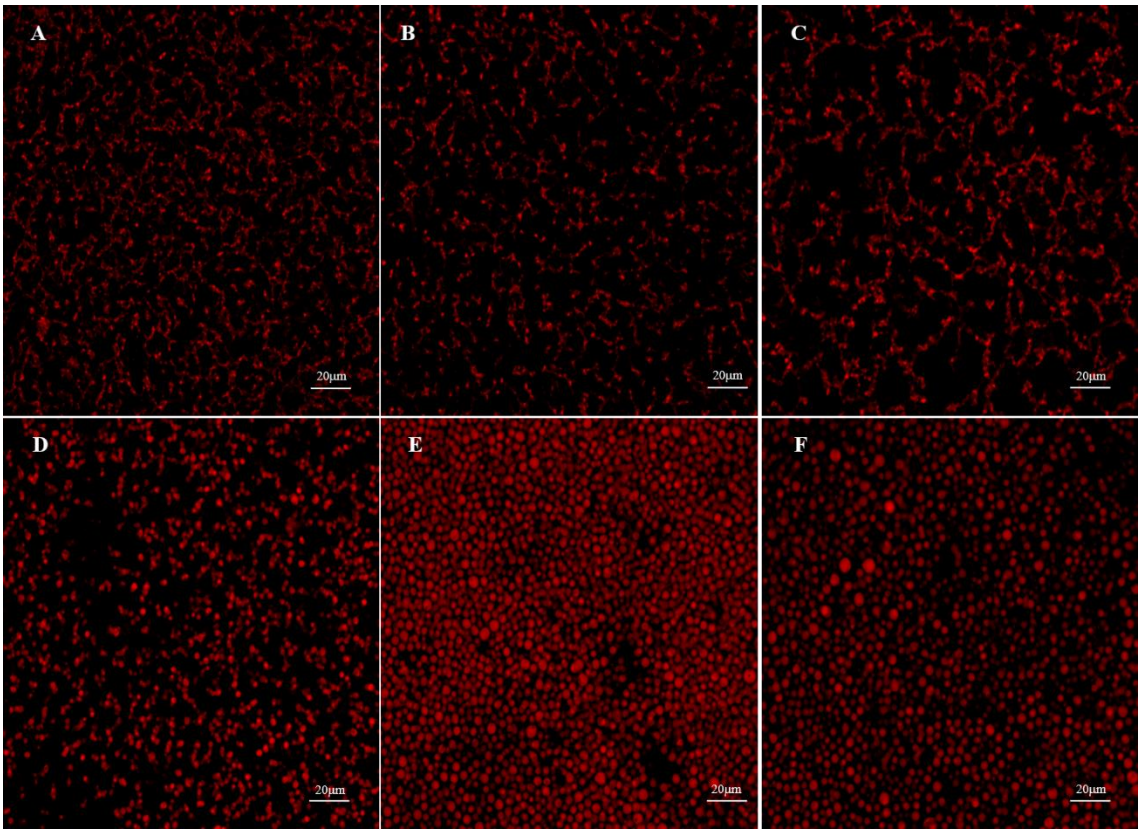

Figure 6

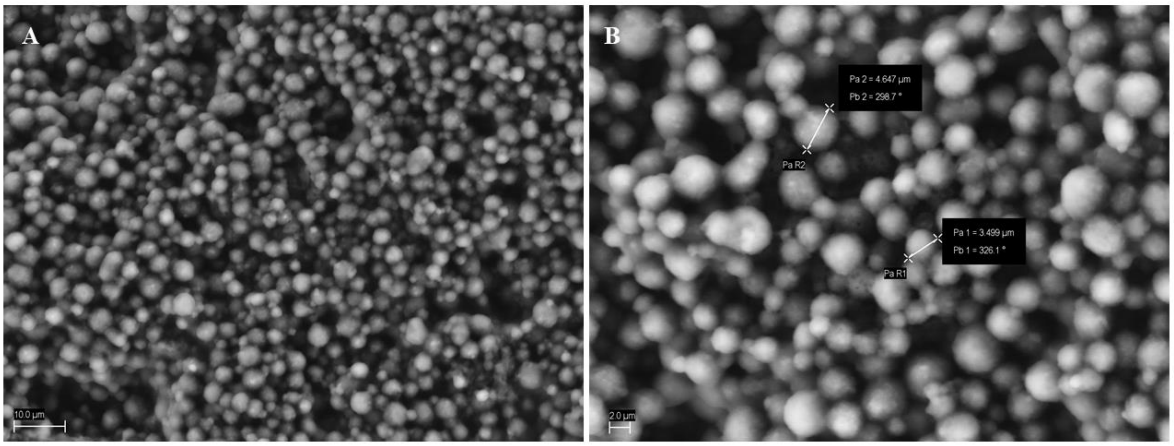
A
10.0 µm
B
Pa 2 = 4.647 µm
Pb 2 = 298.7 °
Pa R2
Pa 1 = 3.499 µm
Pb 1 = 326.1 °
Pa R1
2.0 µm

Table 1: Zeta potential (ζ) measurement of NaCAS, TG, and TG-NaCAS mixtures at 25 °C

C_{NaCAS} (g/100 g)	C_{TG} (g/100 g)	ζ (mV)
0.00	0.10	-19.8 ± 0.7[c]
0.00	0.30	-19.8 ± 0.7[c]
0.00	0.50	-19.8 ± 0.7[c]
3.00	0.00	-28.8 ± 1.2[a]
3.00	0.10	-22.3 ± 1.4[b]
3.00	0.30	-14.7 ± 0.5[d]
3.00	0.50	-10.7 ± 0.4[e]

*Mean value ± standard deviation (n=5).
Means within the same column following by different letters are significantly different ($p < 0.05$).

Table 2: Time (t_{gel}, s) in which a gel formation was observed, pH value observed at the t_{gel} (pH_{gel}), and G'_{max} (Pa) values of NaCAS and TG-NaCAS acid gels. C_{NaCAS} = 3.0 g/100 g, C_{TG} = 0, 0.05, 0.10, 0.20, 0.30, and 0.50 g/100 g, R = 0.5, and T = 18 °C.

C_{NaCAS} (g/100 g)	C_{TG} (g/100 g)	t_{gel} (s)*	pH_{gel}*	G'_{max} (Pa)*
3.00	0.000	3404 ± 6[b]	4.750 ± 0.014[a]	257.95 ± 2.62[c]
3.00	0.050	3273 ± 130[a,b]	4.735 ± 0.092[a]	260.55 ± 8.70[c]
3.00	0.100	3198 ± 135[a,b]	4.755 ± 0.007[a]	83.63 ± 12.26[b]
3.00	0.200	3402 ± 225[b]	4.720 ± 0.071[a]	68.36 ± 13.12[b]
3.00	0.300	3426 ± 129[b]	4.740 ± 0.028[a]	25.05 ± 1.58[a]
3.00	0.500	2853 ± 76[a]	4.530 ± 0.085[a]	19.01 ± 2.16[a]

*Mean value ± standard deviation (n=2).
Means within the same column following by different letters are significantly different ($p < 0.05$).

Table 3: Firmness (FI, N/mm) and fracture force (FF, N) of TG-NaCAS acid gels. C_{NaCAS} = 3 g/100 g, C_{TG} = 0, 0.05, and 0.10 g/100 g, R = 0.5, and T = 18 °C.

C_{NaCAS} (g/100 g)	C_{TG} (g/100 g)	FI (N/mm)*	FF (N)*
3.00	0.000	0.288 ± 0.002[b]	0.840 ± 0.133[a]
3.00	0.050	0.240 ± 0.021[a]	0.612 ± 0.094[a]
3.00	0.100	0.230 ± 0.013[a]	0.668 ± 0.036[a]

*Mean value ± standard deviation (n=3).
Means within the same column following by different letters are significantly different ($p < 0.05$).

Table 4: Water holding capacity (WHC) of TG-NaCAS acid gels. C_{NaCAS} = 3 g/100 g, C_{TG} = 0, 0.05, 0.10, 0.15, and 0.20 g/100 g, R = 0.5, and T = 18 °C.

C_{NaCAS} (g/100 g)	C_{TG} (g/100 g)	WHC (%)*
3.00	0.00	94.590 ± 0.005^{c}
3.00	0.05	93.142 ± 1.750^{c}
3.00	0.10	92.598 ± 0.660^{c}
3.00	0.15	44.065 ± 2.458^{b}
3.00	0.20	29.122 ± 0.671^{a}

*Mean value ± standard deviation (n=3)
Means within the same column following by different letters are significantly different ($p < 0.05$).

Figure captions:

Figure 1. FTIR spectra of food-grade tara gum (TG). At 812 cm^{-1} in the fingerprint region (900-700 cm^{-1}) correspond to the typical galactomannan peaks. Peaks between 1200 and 900 cm^{-1} (carbohydrate region) is related with stretching vibration of C-O in C-O-H bonds. TG spectrum also shows a band at 1640 cm^{-1}, which is attribute to adsorbed water.

Figure 2. Approach used for the determination of the phase diagrams for TG-NaCAS binary systems in buffer Tris-HCl 10 mM pH 6.80 after 48h at (A) 4 ° C, (B) 18 ° C, and (C) 36 ° C (C). Key: (○) one-phase clear solution, (Δ) one-phase turbid solution and (●) two phase samples.

Figure 3. Images of the segregative phase separation process of TG-NaCAS mixture (C_{NaCAS} 3.0 g/100 g and C_{TG} 0.30 g/100 g) at 18 ° C: (A) 4 min; (B) 10 min; (C) 12 min; (D) 18 min; (E) 24 min; and (F) 40 min. Images obtained by CSLM, objective 20× with 4× zoom. Red zones correspond to the protein-rich phase and the dark ones correspond to the polysaccharide-rich phase.

Figure 4. (A) Development of rheological parameters G' (●) and G'' (○) modulus vs. time for NaCAS sample (3.0 g/100 g) after GDL addition (R = 0.50) at 18 °C. (B) Angular frequency dependence of G' and G'' once system reached the equilibrium.

Figure 5. Microstructure of acid TG-NaCAS gels with different C_{TG} obtained by CSLM after addition of GDL: (A) without TG; (B) C_{TG} = 0.05 g/100 g; (C) C_{TG} = 0.10 g/100 g; (D) C_{TG} = 0.20 g/100 g; (E) C_{TG} = 0.30 g/100 g and (F) C_{TG} = 0.50 g/100 g. Objective 20× with 4× zoom, C_{NaCAS} 3 g/100 g, R 0.5 and 18°C.

Figure 6. Microstructure of acid TG-NaCAS gels (C_{NaCAS} 3 g/100 g, C_{TG} 0.20 g/100 g) obtained by ESEM after addition of GDL (R = 0.50): (A) image with 1000 × zoom, and (B) image with 2000 × zoom.